ELSEVIER

Journal of Photochemistry and Photobiology A: Chemistry 139 (2001) 187–197

Journal of Photochemistry and Photobiology A:Chemistry

www.elsevier.nl/locate/jphotochem

The role of the triplet state on the photobleaching processes of xanthene dyes in a poly(vinyl alcohol) matrix

M. Talhavini[1], W. Corradini, T.D.Z. Atvars*

Instituto de Química, Unicamp, Caixa Postal 6154, 13083-970 Campinas, SP, Brazil

Received 16 August 2000; received in revised form 21 November 2000; accepted 5 December 2000

Abstract

This work presents the results for the temperature dependence of the photobleaching reactions of Fluorescein and Rose Bengal dissolved in poly(vinyl alcohol) in the presence of diethylenetriamine, potassium dichromate and 2-aminoethanethiol hydrochloride. These samples were subjected to a continuous irradiation with a 150 W mercury high pressure arc lamp at a wavelength coincident with the maximum of the dye absorption. The photobleaching processes were described by a double exponential and a mono-exponential function for Fluorescein and Rose Bengal, respectively. Apparent activation energies were calculated using the Arrhenius plots and these values were strongly affected by the presence of additives. Different additives are employed in the studies of the photobleaching reactions of Fluorescein and Rose Bengal in poly(vinyl alcohol) matrices: (a) diethylenetriamine is a quencher of all excited states; (b) potassium dichromate is an electron acceptor complexed with the polymer chains and inhibited the photobleaching; (c) 2-aminoethanethiol hydrochloride is an efficient quencher of the triplet state. The role of these additives upon the photoreaction is discussed.

Keywords: Xanthene dyes; Poly(vinyl alcohol); Photobleaching; Diethylenetriamine; Potassium dichromate; 2-Aminoethanethiol hydrochloride

1. Introduction

Photosensitive materials based on a polymer and a photosensitizable dye have proved essential in development of holographic and planar waveguides. Some of these materials were composed of polymers, such as poly(vinyl alcohol) (PVA), poly(acrylic acid) (PAA) [1] and poly(methyl methacrylate) (PMMA) [2]; an electron-donor or acceptor compound such as potassium dichromate [3] or iron chloride [4]; and, in some cases, an organic dye was also included. Examples of dyes incorporated into the polymeric materials are spiropyran [2] and azo-dyes [5] for erasable holograms and xanthene dyes [6] for permanent holograms. Successful applications of polymer/dye systems were controlled by changes of the refractive index of the irradiated samples and by symmetry of the light diffractogram patterns [7,8].

Several strategies have been defined in studies of photobleaching processes of xanthene dyes. In some cases, the major interest is the dye photostabilization, when the dyes are employed as laser sources or as dyes for immunoassays [9,10]. In opposition, if the desired system is employed as holographic recording materials, an irreversible photobleaching reaction must take place [6,8]. Therefore, in the case of immunoassay fluorescence microscopy, fluorescein stabilization was successfully achieved by adding a triplet quencher such as the 2-aminoethanethiol hydrochloride [9,10] while the photobleaching reaction can be enhanced by adding an electron-donor compound [11,12].

Thus, photobleaching processes of xanthene dyes have been studied for different purposes. Fundamental studies focus on the mechanisms of reactions in several media, the role of oxygen in the whole processes was evaluated [11,12] and the quantum yield of the photobleaching reaction was discussed in terms of its dependence on the presence of an electron-donor group. The photoreaction of these dyes dissolved in PVA was dependent on several factors, including the electron transfer ability from the polymer to the dyes; the dye concentration; the temperature; and the polymer relaxation processes [13,14]. The quantum yield of the photobleaching reaction of these dyes in dichromated/PVA was drastically reduced even in the presence of an extrinsic electron-donor specimen (diethylenetriamine) [6]. The effect of amines on the xanthene photobleaching reaction was strongly dependent on their concentration; at low concentration, amines are effective electron-donor specimens, enhancing the photobleaching reactions of the dyes, but

* Corresponding author.
E-mail address: tatvars@iqm.unicamp.br (T.D.Z. Atvars).
[1] Permanent address: Instituto Nacional de Criminalística, Departamento de Polícia Federal, SAIS, lote 07, quadra 23, 70000-000 Brasília, DF, Brazil.

1010-6030/01/$ – see front matter
PII: S1010-6030(00)00426-3

they act as quenchers of the excited electronic singlet state when present in high concentration and, consequently, they may also be able to inhibit the photochemical reactions [11,15]. The quantum yield of xanthene bleaching can also be modified by potassium dichromated/PVA or PAA since a photoelectron transfer reaction of the polymer producing a photoredox process ($Cr^{(VI)} \rightarrow Cr^{(III)}$ and cross-linked polymer) is highly efficient [16].

In previous studies [17–19], we demonstrated by epi-fluorescence microscopy that Fluorescein was useful for "in situ" chemical analysis of polymer blends. It was also noted that polymer blend miscibility may be studied by non-radiative energy transfer of anthracene to Fluorescein when both dyes were dissolved in poly(vinyl alcohol)/poly(vinyl acetate) blends [20]. However, similar to the immunoassay studies, this dye suffered photobleaching during the microscope illumination and the studies must be limited to short exposition periods (a few minutes).

Thus, the present work is an attempt to quantify the reaction kinetics of Fluorescein and Rose Bengal dissolved in PVA and to compare the relative efficiencies of the bleaching processes in the presence and the absence of some additives in order to improve the dye photostability. Although, some studies treating the photobleaching of these dyes in PVA were already published, detailed data related to the effects of additives/dyes on the polymer morphology are not described [1–7,13–14]. In addition, the rate constants for the photobleaching reaction in the presence of additives have also not been reported, at least to our best knowledge.

2. Experimental

Poly(vinyl alcohol) (PVA) (Aldrich Chemical Co.) $M_w = 124,000\,g\,mol^{-1}$, 87–89% hydrolyzed, was used as received. It is a semi-crystalline polymer with a crystallinity index, determined by X-ray diffraction, of 43%; a glass transition temperature at ca. 343 K and a melting point at ca. 453 K [17–19].

Fluorescein (FL) and Rose Bengal (RB) (Aldrich Chemical Co., analytical grade) were recrystallized from an ethanolic solution, dried under vacuum and stored in the dark. The dyed PVA films were prepared as described elsewhere [17–19]. The dye concentration was defined as $10^{-3}\,mol\,l^{-1}$. All of the doped films have good optical transparency and their thickness range was ca. 58–60 μm.

The additives incorporated into the dye/PVA films were: 2-aminoethanethiol hydrochloride (TIOL) 98%; diethylenetriamine (DTT); and potassium dichromate ($Cr^{(VI)}$), all purchased from Aldrich Chemical Co. Both TIOL and DTT were used as received while potassium dichromate was twice recrystallized from a saturated aqueous solution. The concentration of additives was ca. $1–10^{-2}\,mol\,l^{-1}$.

Terbium chloride (Tb) (99.5%) and benzophenone were purchased from Aldrich Chemical Co and were used as received.

The thermal properties of all samples were measured calorimetrically using a Dupont 2910 differential scanning calorimeter (d.s.c.) that was controlled by a TA module 2000 and a data analysis system. Temperature calibration was performed using indium ($T_m = 429.60$ K) as standard. The heating cycles were conducted at a heating rate of 10 K/min, with a sample size between 10 and 15 mg in standard aluminum pans. A temperature range of 293–493 K using liquid nitrogen cooling was used. Following the convention used in other thermal analysis studies, the glass transition was taken as the temperature at which the heat capacity reached one-half of the entire step change and it was measured by the midpoint method [21]. The melting temperature was taken as the maximum of the endothermic peak.

The photobleaching studies of dyed films were performed using the sample experimental setup described earlier [22] with the samples irradiated at $\lambda_{ex}(FL) = 445$ nm and $\lambda_{ex}(RB) = 490$ nm. Fluorescence intensity was measured at $\lambda_{em}(FL) = 515$ nm and $\lambda_{em}(RB) = 590$ nm. The experimental data were collected at intervals of 5 or 10 s during a maximum of 3 h, depending on the reaction rate. This procedure was repeated for several temperatures from 260 to 400 K, which were provided by a digital temperature controller (Scientific Instruments, model 9650) with a precision of ±0.5 K. Since the additive absorption was not coincident to dye absorption or emission, the reaction rate is considered only dependent on the efficiency of the dye excitation processes.

Measurements of excitation and prompt fluorescence at room temperature and delayed fluorescence and phosphorescence spectra at 77 K were performed using a PTI LS100 (Photon Technology International) spectrofluorimeter in the steady-state mode. Delayed fluorescence and phosphorescence decay curves were recorded after excitation with a pulsed xenon lamp. Prompt fluorescence decay curves were generated using pulsed nitrogen lamps, selecting an appropriate delay channel. Standard software supplied by the manufacturer was employed for the convolution of the lamp pulse and the emission decay signal.

3. Results and discussion

3.1. Effect of additives upon the properties of the PVA matrix

Melting points and glassy transition temperatures of the PVA matrix with and without additives were determined by d.s.c. (Fig. 1). Curve profiles for PVA and PVA/FL are virtually the same (at least with the concentrations employed in this work) and thus, the presence of dyes in the polymer matrices does not modify the PVA melting temperature. Nevertheless, the endothermic melting peak of the PVA samples containing the xanthene molecules is broadened, demonstrating that strong dye–polymer interaction

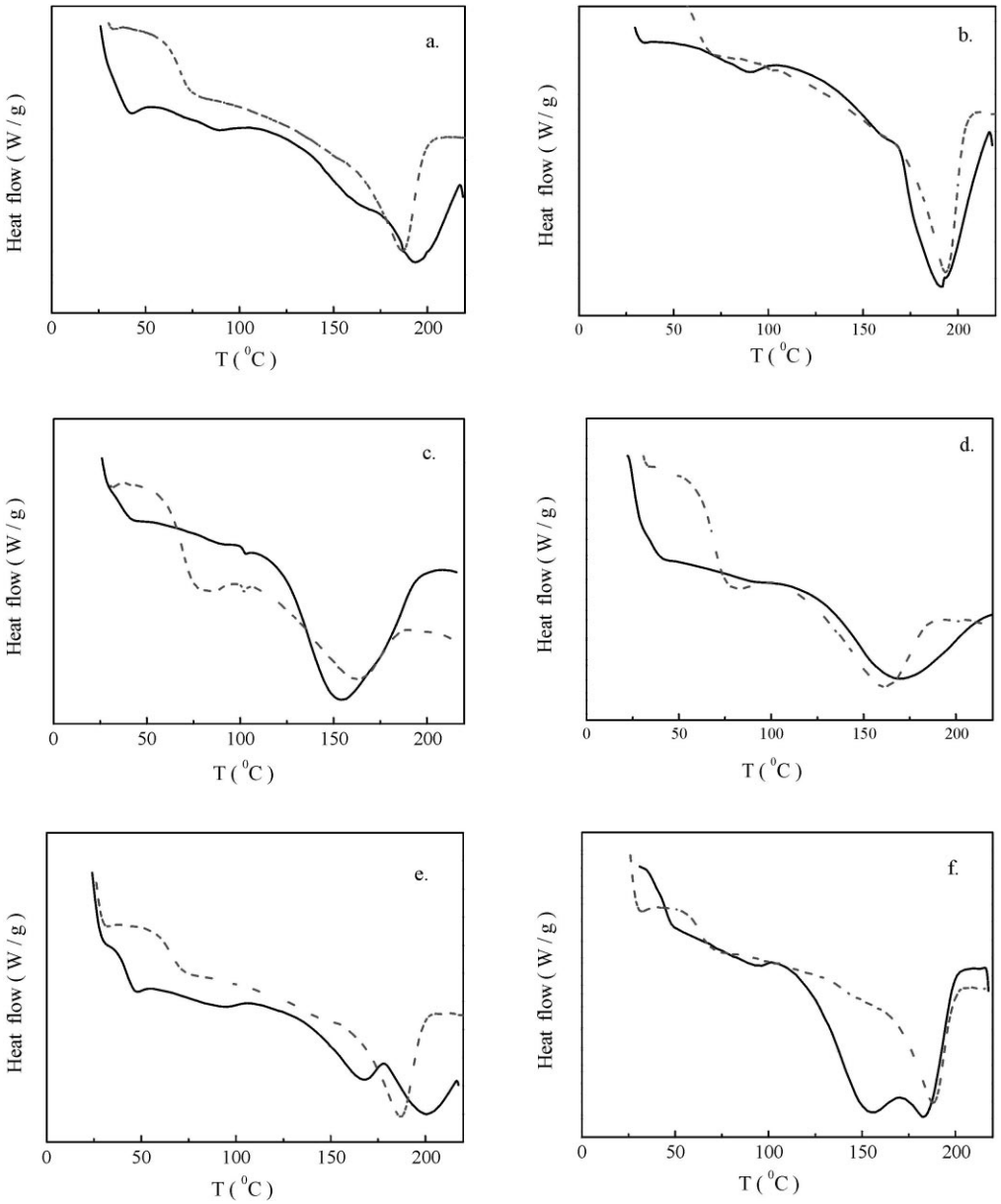

Fig. 1. Differential scanning calorimeter thermograms for: (a) PVA-homopolymer/FL; (b) PVA/DTT/FL; (c) PVA/potassium dichromate; (d) PVA/potassium dichromate/FL; (e) PVA/TIOL and (f) PVA/TIOL/FL. Heating rate, 10 K min^{-1}. First (—) and second (---) scans. Dye concentration is 10^{-3} mol l^{-1}.

by hydrogen bondings is interfering with the crystallization process of the polymer chains.

Changes of the relative crystallinity degree, compared to PVA-homopolymer, are calculated using the melting enthalpies for the second heating scan:

$$\chi_R(\text{d.s.c}) = \frac{\Delta H_m^0}{\Delta H_m^S} \quad (1)$$

where ΔH_m^0 and ΔH_m^S are the melting enthalpies measured for PVA-homopolymer (PVA) and PVA-additives (S), respectively. These values are listed in Table 1.

Remarkable effects on the polymer crystallization process are produced when potassium dichromate and TIOL are incorporated into PVA and PVA/dye materials (Fig. 1). Potassium dichromate induces a decrease of both the melting temperature and the degree of crystallinity of PVA semi-crystalline polymer, in addition to an important broadening of the endothermic peak (Fig. 1). Crystallization processes forming crystals with broad size distribution and/or of smaller size crystals explain the broadening of d.s.c. peaks [21].

Different from potassium dichromate, PVA crystallization in presence of TIOL leads to a d.s.c. profile with two crystallization peaks in the first heating cycle of the sample. The second heating cycle eliminates the lower temperature peaks, suggesting that the TIOL confers a certain mobility to the amorphous phase during the heating cycle, reordering

Table 1
Glass transition, melting temperature and crystallinity ratio of PVA, PVA-additives and PVA-additives/Fluorescein[a] from the d.s.c. curves in Fig. 1

Samples	First heating		Second heating		
	T_g (°C)	T_m (°C)	T_g (°C)	T_m (°C)	χ_R (d.s.c.)[b]
PVA	53	188	71	186	1.0
PVA/FL	66	160/193	68	187	0.8
PVA/DTA/FL	80	160/191	62	194	1.6
PVA/$Cr^{(VI)}$	70	153	68	160	2.8
PVA/$Cr^{(VI)}$/FL	80	168	68	160	2.6
PVA/TIOL	44/104	166/201	65	187	1.4
PVA/TIOL/FL	44	160/183	63	188	1.3

[a] Fluorescein concentration is 10^{-3} mol l^{-1}.

[b] χ_R(d.s.c) $= \Delta H_m^0/\Delta H_m^S$ is the relative crystallinity where ΔH_m^0 and ΔH_m^S are the melting enthalpies measured for PVA-homopolymer (PVA) and PVA-additives (S), respectively, from the second d.s.c. heating curves.

the polymer chains [21] (Fig. 1). Although, the sample containing DTT exhibits a smaller degree of crystallinity the effect upon the melting crystallization temperature is less important (Table 1).

Glass transition temperatures were also determined from the second heating scan curves of the d.s.c., in order to eliminate the endothermic peak overlapped with the glass transition [21]. Values for glass transition temperatures are listed in Table 1 and they are usually lower for additived compared to non-additived polymer samples.

3.2. Spectroscopic properties of the xanthene/PVA/additive systems

The fluorescence spectra of xanthene dyes in PVA are strongly dependent on the dye concentration. At very low concentration it mimics the spectrum of xanthene in a water/ethanol (85/15 v/v%) solution. The spectral maximum is centered at 505 nm for FL [13,23]. The absorption band may be attributed to neutral specimens in the electronic ground state and to monoanion/dianion specimens in emission [24]. The emission spectrum of 10^{-3} mol l^{-1} FL in PVA exhibits a small red shift compared to the solution, with the band peak centered at 520 nm, resulting in an efficient self-absorption and re-emission processes (Fig. 2) [25]. Time resolved spectroscopy reveals the presence of an efficient self-quenching process, that is, explained by the partial dimerization of the dye undetected by steady-state fluorescence spectroscopy [13]. The fluorescence of RB in PVA is assigned to its dianion species.

The temperature dependence of the fluorescence spectra of FL in PVA has already been reported [22]. A monotonic red shift from 505 to 520 nm is obtained for 10^{-3} mol l^{-1} FL/PVA with the increase of the temperature attributed to the solvent cage relaxation around the excited state fluorescence molecule. Similar results were obtained for RB in PVA (Fig. 2).

The influence of some additives upon the fluorescence spectra is also noted for PVA/xanthene/additive samples. The fluorescence spectrum is sharper in presence of DTT (an amine) and there is a red shift of the whole spectrum, compared to non-additived PVA. This is explained by the increase of the basicity of the medium and hence, xanthene dissociation equilibrium is shifted towards the dianion specimens of the dye [24]. No spectral shifts were observed for the xanthene emissions in the presence of potassium dichromate.

TIOL is supposed to be an efficient quencher for the triplet state without interference from the excited singlet state. This assumption is confirmed by exploratory experiments of phosphorescence quenching measurements performed under both steady-state and time-resolved conditions of some strongly phosphorescent and fluorescent specimens in solutions containing TIOL:

1. phosphorescence emission is quenched and the phosphorescence lifetime decreases for a degassed solution of 5.5×10^{-3} mol l^{-1} of benzophenone in ethanol containing TIOL (10^{-3} mol l^{-1}) (at 77 K) (Fig. 3a, Table 2);
2. phosphorescence emission is quenched and phosphorescence lifetime decreases (at room temperature) for a solution of 5.5×10^{-3} mol l^{-1} of terbium chloride in water containing TIOL (10^{-3} mol l^{-1}) (Fig. 3b, Table 2);
3. fluorescence intensity, at room temperature, of 3×10^{-3} mol l^{-1} of FL in ethanol remains constant with successive additions of TIOL (5×10^{-4}–10^{-2} mol l^{-1}) (Fig. 3c);

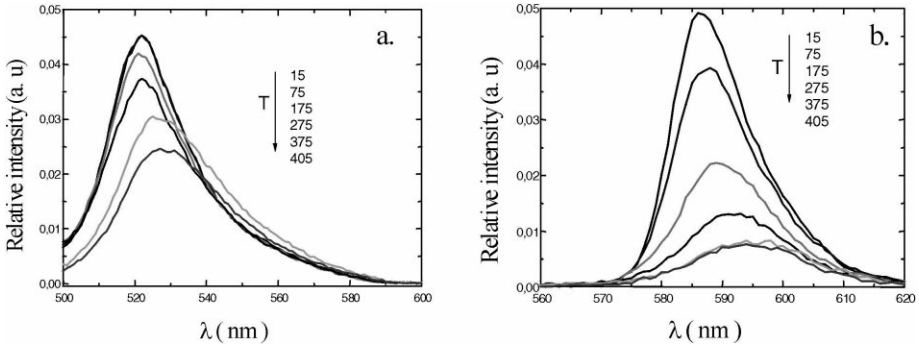

Fig. 2. Fluorescence spectra at several temperatures for: (a) PVA/FL and (b) PVA/RB. Dye concentration is 10^{-3} mol l^{-1}.

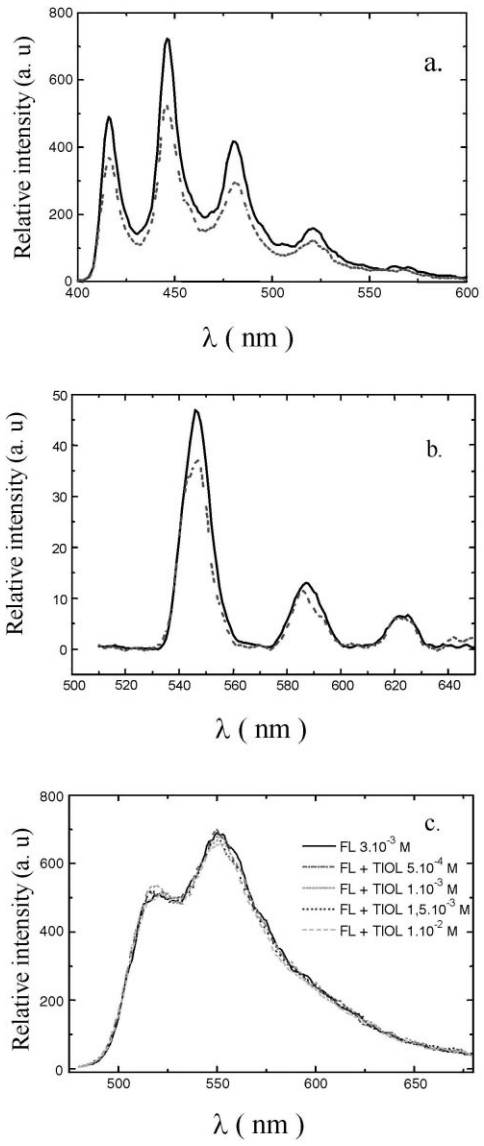

Fig. 3. Phosphorescence spectra in the presence (---) and absence (—) of TIOL of: (a) 5.5×10^{-3} mol l^{-1} benzophenone/ethanol at 77 K; (b) 5.5×10^{-3} mol l^{-1} terbium chloride/water at room temperature. (c) Fluorescence spectra of 3×10^{-3} mol l^{-1} fluorescein/ethanol in presence of several amounts of TIOL.

4. decay curves for the phosphorescence and delayed fluorescence lifetimes decreased for degassed solutions of RB in ethanol (1×10^{-3} mol l^{-1}) at 77 K revealed quenching processes of the dye by the TIOL (10^{-3} mol l^{-1}) (Fig. 4a, Table 2);
5. phosphorescence decay curves for RB in PVA (10^{-3} mol l^{-1}) at 77 K also reveals that the lifetime is reduced by TIOL (Fig. 4b, Table 2).

Therefore, we observe simultaneously, a decrease of phosphorescence intensity and lifetime, for samples containing TIOL, that is characteristic of quenching processes of the triplet state (Table 2). Nevertheless, in spite of the quenching of the triplet state, the fluorescence intensity remains constant for an ethanolic solution of FL after successive additions of TIOL (Fig. 3c) confirming its specificity as quencher for the triplet state [9,10].

3.3. Kinetic description of the photobleaching reactions

Experimental curves for the photobleaching reaction under continuous irradiation of the samples, for both Fluorescein and Rose Bengal (10^{-3} mol l^{-1}) in PVA matrices were obtained at several temperatures in the absence and in the presence of additives (Figs. 5 and 6). The temperature range is chosen to cover values below and above the PVA glass, transition ca. 340 K.

These experimental curves were analyzed by a sum of two or more exponential functions to fit the experimental data of fluorescence intensity versus time:

$$I_F(t) = C + \sum A_i \exp\left(\frac{-t}{\tau_i}\right) \quad (2)$$

where $I_F(t)$ is the time-dependent fluorescence intensity, proportional to the electronic ground state population; A_i the pre-exponential factor interpreted as an amplitude factor proportional to the relative contribution of each rate constant, independent of the temperature; C the integration constant; and τ_i the lifetime defined as the time necessary for the emission to reach 1/e of the initial value.

The requirement for, at least, a bi-exponential function for the kinetic description of processes in polymer matrices is interpreted by the presence of at least two sorption sites for the guest molecules in semi-crystalline polymer matrices [26,27]. The existence of two rate constants can be explained by a two phase model where the dye molecules are distributed into two types of sites: one, containing isolated molecules in close contact with the polymer chains, that is

Table 2
Decay constants (τ, ms) for benzophenone, terbium chloride and Rose Bengal (the concentrations are referred to the dye)

Samples	τ_{Ph} (ms) without TIOL	τ_{Ph} (ms) with TIOL
Benzophenone/ethanol[a], 5.5×10^{-3} mol l^{-1}	5.2	3.9
Terbium chloride/water[b], 5.5×10^{-3} mol l^{-1}	0.33	0.17
Rose Bengal/ethanol[a], 1×10^{-3} mol l^{-1}	0.71	0.50
Rose Bengal/ethanol[a], 10^{-3} mol l^{-1} (delayed fluorescence)	1.91	1.18
Rose Bengal /PVA[b], 10^{-3} mol l^{-1}	0.26	0.12

[a] 77 K.
[b] Room temperature.

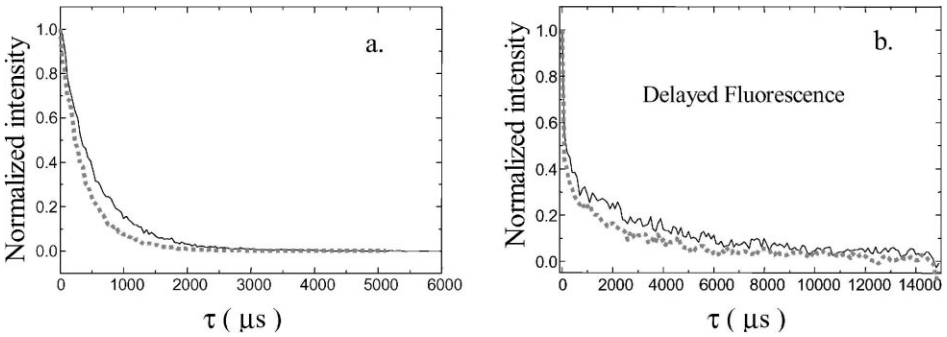

Fig. 4. (a) Phosphorescence decay and (b) delayed fluorescence decay of 10^{-3} mol l^{-1} Rose Bengal in ethanol at 77 K. Absence (—) and presence (---) of TIOL.

responsible for the slower process, and another, containing molecules that can interact by themselves. In the last case the D–D mechanism for photoreaction should be responsible for the faster reaction [13].

Rate constants and apparent activation energies are calculated by fitting the experimental data with a multi-exponential function (2) (Figs. 5 and 6). The goodness of the fits for both mono- and bi-exponential functions are analyzed taking into account the two parameters: the χ^2 values and the distribution of residuals. As a general behavior, we observe that, while the mono-exponential function provides reasonable fit for RB photobleaching reactions, for FL a bi-exponential function is necessary. Thus, two rate constants are determined, one for a faster and other for a slower photobleaching process. The contribution of the normalized weight factors for the faster (A_1) and slower (A_2) processes depends on the temperature; the slower processes exhibit the major contribution at lower temperatures, while the weight factor for the faster component becomes virtually equal above the glass transition temperature.

Apparent activation energies for the photobleaching process are calculated using the Arrhenius equation for rate constants ($k_i = 1/\tau_i$ in Eq. (2)) at several temperatures:

$$k = A \exp\left(\frac{-E_a}{RT}\right) \quad (3)$$

where A and E_a are the frequency factor and the apparent activation energy, respectively.

The slower photobleaching process for RB compared with FL in the non-additive polymer matrix is attributed to an efficient triplet–triplet annihilation that competes with the photoreaction and quenches the electronic excited state. Values determined for the apparent activation energies are 85 kJ mol^{-1} for RB (mono-exponential) and 21 and 7 kJ mol^{-1} for FL (a bi-exponential model) (Table 3).

We performed similar experiments using the dye/PVA/DTT system that contains 1 mol l^{-1} electron-donor additive. The best-fit of the experimental data is obtained using bi-exponential and mono-exponential functions for samples with 10^{-3} mol l^{-1} FL and RB, respectively. The pre-exponential weight factors A_1 (for the faster process) and A_2 (for the slower process) exhibit a similar temperature dependence as for FL/PVA; at lower temperatures the dominant component is the slower rate, while at higher temperatures the faster process predominates. Moreover, lower apparent activation energies are always determined in presence of DTT (Figs. 5 and 6) (E_a(FL) = 17 and 25 kJ mol^{-1} and E_a(RB) = 70 kJ mol^{-1}) compared to the dyes dissolved in non-additived homopolymer (Table 3).

The photobleaching reactions were also studied for dye/PVA/potassium dichromate (electron-acceptor additive) and dye/PVA/TIOL (a triplet quencher) (Figs. 5 and 6). Compared to the non-additived samples, the apparent activation energies are 40 and 100% higher, respectively, for potassium dichromate and TIOL additived samples with FL (Table 3).

3.4. Mechanism of photobleaching reactions

The analysis of the influence of additives upon dye stabilization is based on the kinetic scheme already proposed by Lindqvist [24] and subsequently modified by Song et al. (Scheme 1) [9,10]. As we can see in this scheme, the triplet is postulated as the reactive electronic state (reactions a–i). Therefore, we will consider the relative importance of the following pathways for the photobleaching processes [28]:

Table 3
Apparent activation energies, E_a (kJ mol^{-1}), from Figs. 5 and 6, for Fluorescein (FL) and Rose Bengal (RB) in PVA with and without additives[a]

	E_a (faster component)	E_a (slower component)
PVA/FL	7	21
PVA/FL/DTT	17	25
PVA/FL/Cr$^{(VI)}$	29	29
PVA/FL/TIOL	24	47
PVA/RB	85	85
PVA/RB/DTT	70	70
PVA/RB/Cr$^{(VI)}$	97	97
PVA/RB/TIOL	108	108

[a] Dye concentration is 10^{-3} mol l^{-1}.

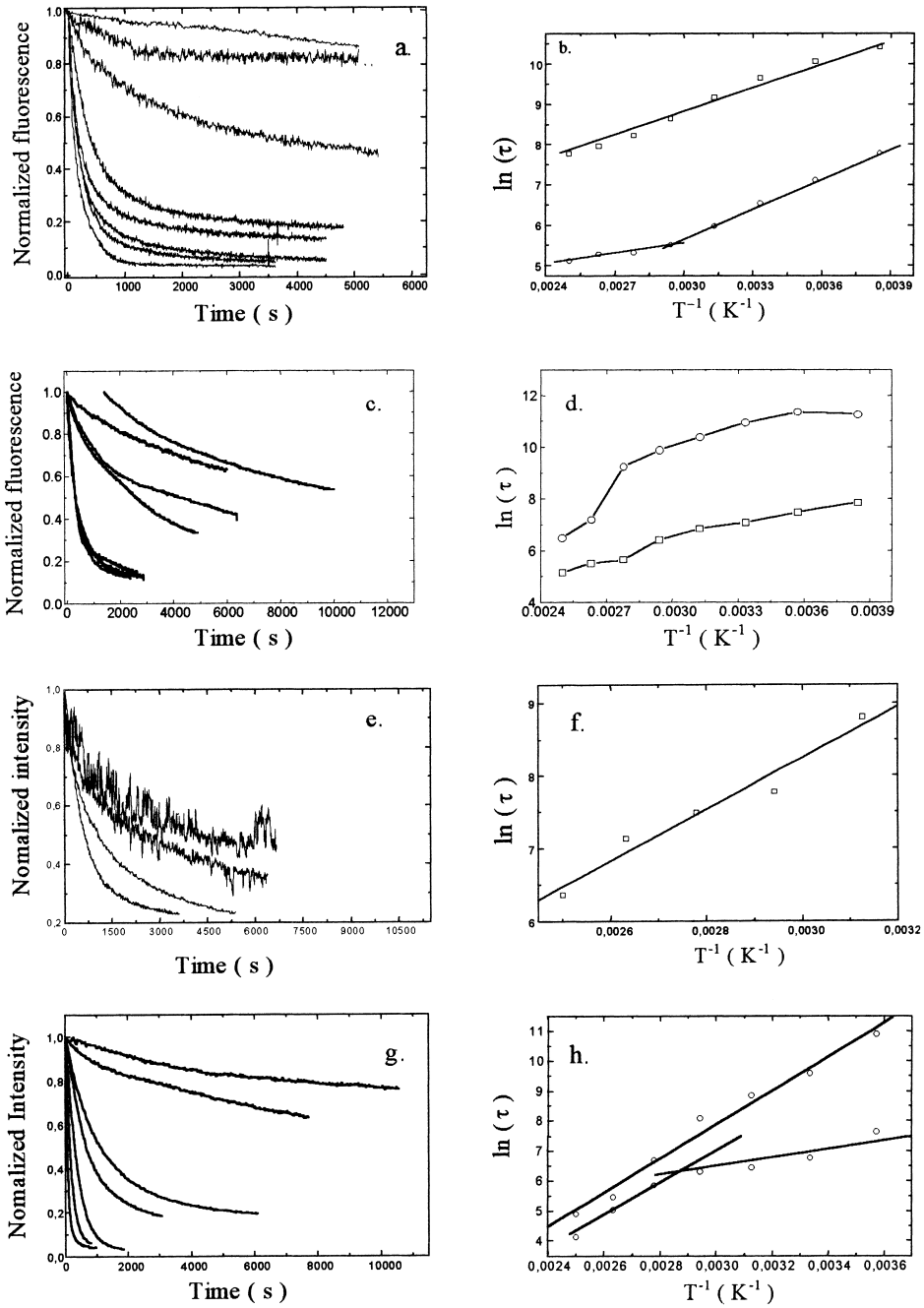

Fig. 5. Photobleaching curves (left side) and the Arrhenius plots, $\ln(\tau_{Fl}) \times T^{-1}$, (right side) for: (a) and (b) PVA/FL (temperatures 280–400 K); (c) and (d) PVA/FL/DTT (temperatures 280–400 K); (e) and (f) PVA/FL/$Cr^{(VI)}$ (temperatures 320–400 K), and (g) and (h) PVA/FL/TIOL (temperatures 280–400 K).

1. triplet quenching (reactions a–c) leading to dye deactivation without photobleaching reactions;
2. D–D mechanism (reaction d) producing either the $\mathbf{D}^{\bullet}$ or $\mathbf{DH}^{\bullet}$ intermediates and dye bleaching that describes the effect of concentration upon the reaction rate;
3. the photobleaching reaction in the presence of either an electron or a hydrogen donor group, to produce $\mathbf{D}^{\bullet}$ or $\mathbf{DH}^{\bullet}$ (reactions e–g); these are important steps for the present work;
4. dehalogenation reactions after dye excitation are important pathways for RB (omitted in the scheme).

Reactions (h) and (i) are neglected under our experimental conditions since the experiments are performed under vacuum (absence of O_2) and with continuous pumping.

Thus, in very diluted FL or RB/PVA samples the photoreaction is a slower process either in presence of an electron (e) or hydrogen (f) donor group because the D–D mechanism is absent, as we described previously [14]. At higher

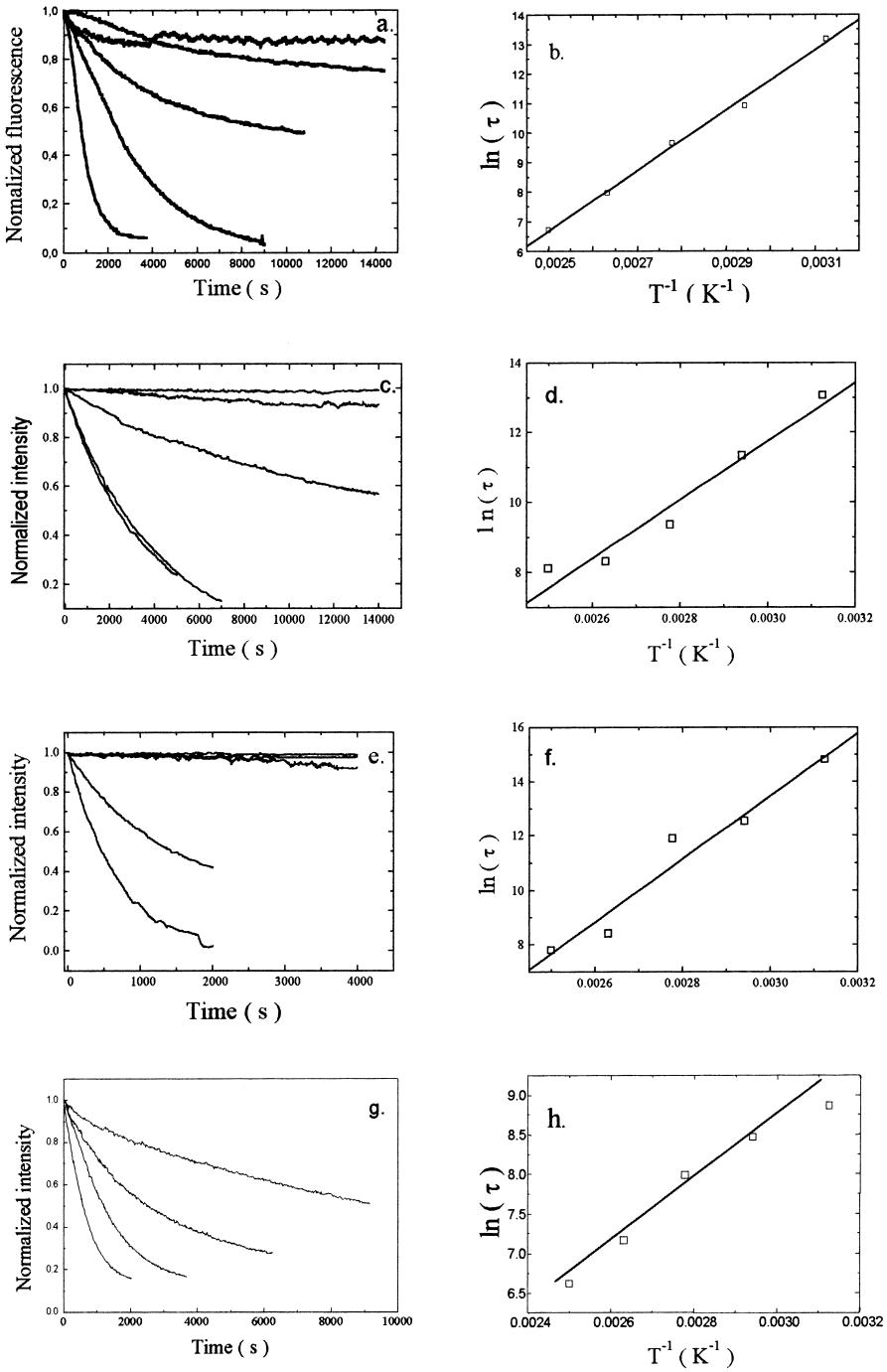

Fig. 6. Photobleaching curves (left side) and the Arrhenius plots, $\ln(\tau_{RB}) \times T^{-1}$, (right side) for: (a) and (b) PVA/RB; (c) and (d) PVA/RB/DTT; (e) and (f) PVA/RB/$Cr^{(VI)}$; and (g) and (h) PVA/RB/TIOL (temperatures 320–400 K).

concentrations, the mechanism for fluorescein photobleaching is bi-exponential and the D–D pathway predominates over other steps. This D–D pathway must be controlled by diffusion and thus, it becomes more effective at $T > T_g$ (PVA glass transition temperature). At $T < T_g$ the matrix is almost completely frozen, a non-diffusive D–D mechanism predominates and fluorescence quenching is observed.

It is well known that intersystem crossing is more efficient for RB than for FL [25,29]. Although, the rate constant for the intersystem crossing process for these dyes in a PVA matrix in unknown, data reported for RB in methanol indicate that k_{isc} (RB) is at least 2 orders of magnitude faster than for FL [25]. If the photobleaching rate constants are only dependent on the triplet state population, faster photobleaching should be expected for RB. Assuming that the rate constants for FL and RB radiative processes are similar (a few nanoseconds for fluorescence and milliseconds for phosphorescence emission decays, respectively),

$T^* \longrightarrow S$	(k_1 radiationless deactivation)	(a)
$T^* + T^* \longrightarrow T^* + S$	(k_2 triplet-triplet quenching)	(b)
$T^* + S$ or $M \longrightarrow S + S$ or M	(k_3 triplet quenching)	(c)
$T^* + T^* \longrightarrow DH^{\bullet} + D^{\bullet}$	(k_4 electron transfer)	(d)
$T^* + M \longrightarrow DH^{\bullet} + D$	(k_5 electron transfer)	(e)
$T^* + D^{\bullet} \longrightarrow S + D^{\bullet}$	(k_6 triplet quenching by X)	(f)
$T^* + DH^{\bullet} \longrightarrow S + DH^{\bullet}$	(k_7 triplet quenching by R)	(g)
$T^* + O_2 \longrightarrow S + O_2$	(k_8 physical quenching by O_2)	(h)
$T^* + O_2 \longrightarrow D^{\cdot} + HO_2$ or O_2^-	(k_9 chemical quenching by O_2)	(i)

Scheme 1. Photobleaching pathways for Fluorescein and Rose Bengal [9,10,24] (S is the molecule in the electronic ground state, $\mathbf{D}^{\bullet}$ and $\mathbf{DH}^{\bullet}$ are the semioxidized and protonated semireduced molecules, respectively; **M** is an electron or hydrogen donor group).

the slower RB/PVA photobleaching rates compared with FL/PVA should involve subsequent slower pathways after the population of the triplet state. Moreover, while RB/PVA photochemical rate constants are not altered by dye concentration, different from the FL/PVA system, the D–D mechanism leading to the bleached specimens should be negligible compared with the faster radical recombination inside the polymer cage. Whatever these steps are, we may conclude that while the D–D mechanism is efficiently producing the photobleaching process of FL, they are probably producing an efficient quenching of the triplet state recovering non-excited RB.

The effect of additives (potassium dichromate, DTT and TIOL) upon the apparent activation energies for the photobleaching processes is analyzed considering their abilities as: (1) electron-donors for xanthene dye in the triplet state, increasing the photobleaching rate constants; (2) quencher of the dye in the electronically excited singlet or triplet states, decreasing the photobleaching rate constant; and (3) plasticizers for the polymer matrix that increase polymer chain mobility.

3.4.1. Effect of the amine, DTT

Amines are known as efficient quenchers of xanthene fluorescence emission that depend on both the relative ionization potential and concentration. The Stern–Volmer constant (K_{SV}) for the quenching process of RB by DTT in ethanolic solution is $K_{SV} = 1.5\,(\mathrm{mol\,l^{-1}})$ and the process becomes more efficient at higher amine concentrations ($> 5 \times 10^{-2}\,\mathrm{mol\,l^{-1}}$). The quenching of the dye triplet state is also appreciable at high amine concentration, occurring by a charge-transfer mechanism [30]:

$$^3\mathrm{Dye}^* + \mathrm{Am} \rightarrow \mathrm{Dye}^{-\bullet} + \mathrm{Am}^{+\bullet} \qquad \text{(j)}$$

where Am is the amine [30].

It is also postulated that while the photobleaching of xanthene dyes involves either semi-reduced or semi-oxidized specimens, in presence of amines only the semi-reduced eosin radical is produced [12]. Photoreduction produces two leuco analogues: the dihydro-derivative and the cross-coupled product involving an amine radical and a dye radical anion [12,31]. Assuming that the semireduced dye is the principal specimen formed in the presence of amines, reactions d, e and g are important pathways for the bleaching process at lower concentrations ($<0.5\,\mathrm{mol\,l^{-1}}$). Nevertheless, at higher concentrations such as those used in the present work, pathway c is the most efficient quenching process for both singlet and triplet states [32]. The lower efficiency of the photobleaching reaction, represented by higher values of the apparent activation energies (Table 3) is attributed to the ability of the amine to be a general quencher for the excited states, in opposition to its electron-donor ability that should enhance the reaction.

In addition to the ability of amines to be quenchers of excited states, they can also act as PVA plasticizers, since they decrease both the glass transition temperature and the PVA crystallinity ratio (Fig. 1, Table 1). The decrease of the glass transition temperature is confirmed by the slope change of the rate constant in the Arrhenius plots, compared with the non-additived sample (Fig. 5).

3.4.2. Effect of the potassium dichromate

In opposition to amines, potassium dichromate is an electron-acceptor additive. Upon photoexcitation it can undergo photoreduction from $Cr^{(VI)}$ to $Cr^{(III)}$ in a PVA matrix by an electron-transfer reaction with polymer oxidation (reaction k) [6,30,32]. In addition, d.s.c curves reveal that the $Cr^{(VI)}$ is complexed with the PVA. Thus, the presence of both specimens in the PVA matrix creates a competition by the electron supplied by the polymer and inhibits the photobleaching reaction. The increase of the apparent activation energy observed for both dyes (Figs. 5 and 6, Table 3) is explained by this competitive reduction of $Cr^{(VI)}$ to $Cr^{(III)}$. Thus, an additional reaction in dichromated-PVA samples must be considered:

$$^3\text{Dye}^* + \text{Cr}^{(\text{VI})} + \text{polymer} \rightarrow \text{Dye}^{+\bullet} + \text{Cr}^{(\text{III})} + \text{oxidized polymer} \quad \text{(k)}$$

It is noteworthy that the kinetic curves for FL/PVA may be simulated by a mono-exponential function and the corresponding apparent activation energy is larger than that obtained for the slower processes in non-additived PVA. This result confirms that the photobleaching processes is inhibited by chromium complexation with the polymer chain.

3.4.3. Effect of TIOL

The larger apparent activation energies for the photobleaching reaction of both dyes in PVA/TIOL are attributed to the quenching process of the triplet state (reaction l — quenching of the dye in the triplet state) without any change in the fluorescence emission intensity [9,10] (Figs. 3 and 4):

$$^3\text{Dye}^* + \text{TIOL} \rightarrow \text{Dye} + \text{TIOL} + \text{heat} \quad \text{(l)}$$

Although, this additive produces a decrease of both PVA glass transition and melting temperatures, this effect is less significant for the photobleaching reaction than the efficiency of the triplet state quenching. Similarly, other systems containing Fluorescein, the kinetics are well described by a bi-exponential function, with the faster component of the rate constant exhibiting a slope change at a temperature close to the PVA-glass transition. Above this temperature, the weight factor for the slower process is negligible.

4. Conclusions

Photobleaching kinetics of FL and RB dyes dissolved in an additived PVA matrix were studied at temperatures below and above the PVA glass transition and the experimental curves are analyzed using exponential functions. This approach demonstrates that the apparent activation energy is a useful parameter to evaluate the efficiency of the photobleaching reaction in the presence or absence of extrinsic additives: an electron-donor/excited state quencher, an electron-acceptor and a specific triplet state quencher.

The most important mechanism for the xanthene photobleaching reaction in PVA matrices involves the semi-reduced intermediate producing a leuco-dye, in agreement with the eosin photoreaction and an oxidized polymer [11,12]. The relative importance of the triplet state is clearly demonstrated since TIOL (that is, a specific quencher of the triplet state) induces a process with higher activation energy values.

We also demonstrated that both xanthene dyes (FL and RB) are photostabilized by adding to the PVA matrix; an amine, which acts as a general quencher for the excited states or potassium dichromate which competes with the dye photoreduction reaction.

Fluorescein, in more concentrated samples, exhibited a faster photobleaching process, attributed to dye–dye interaction. The relative importance of this process is strongly dependent on the temperature and it becomes the most important processes above the PVA glass transition temperature. This faster process is absent for RB, probably due to triplet–triplet annihilation leading to the unbleached dye in the electronic ground state. The difference between rate constants for quenching and electron transfer processes should be responsible for the higher photostability of RB in a PVA matrix.

Acknowledgements

T.D.Z. Atvars thanks FAPESP for financial support. M.T. and W.C. acknowledge fellowships from FAPESP and CAPES, respectively. The authors thank Prof. Carol Collins for useful discussions.

References

[1] R.A. Lessard, G. Manivannan, J. Im. Sci. Technol. 41 (1997) 228.
[2] S.S. Xiu, G. Manivannan, R.A. Lessard, Thin Solid Films 253 (1994) 228.
[3] G. Manivannan, G. Lemelin, R. Changkakoti, R.A. Lessard, Appl. Opt. 33 (1994) 3478.
[4] F. Trepanier, G. Manivannan, R. Changkakoti, R.A. Lessard, Can. J. Phys. 71 (1993) 423.
[5] V.P. Pham, G. Manivannan, R.A. Lessard, Opt. Mater. 4 (1995) 467.
[6] G. Manivannan, P. Leclere, S. Semal, R. Changkakoti, Y. Renotti, Y. Lion, R.A. Lessard, Appl. Phys. B-Laser Opt. 58 (1994) 73.
[7] D.H. Liu, G. Manivannan, H.H. Arsenault, R.A. Lessard, J. Mod. Opt. 42 (1996) 639.
[8] G. Manivannan, R. Gangkakoti, R.A. Lessard, G. Maillot, M. Bolte, J. Phys. Chem. 97 (1993) 7228.
[9] L. Song, C.A.G.O. Varma, J.W. Verhoeven, H.J. Tanke, Biophys. J. 70 (1996) 2959.
[10] L. Song, E.J. Hennik, I.T. Young, H.J. Tanke, Biophys. J. 68 (1995) 2588.
[11] D.F. Eaton, in: D.H. Volman, G.S. Hammond, K. Gollnick (Eds.), Advances in Photochemistry, Vol. 13, Wiley/Interscience, New York, 1986, p. 427 and references cited herein.
[12] D.C. Neckers, O.M. Valdes-Aguilera, in: D. Volman, G.S. Hammond, D.C. Neckers (Eds.), Advances in Photochemistry, Vol. 18, Wiley/Interscience, New York, 1993, p. 315, and references cited herein.

[13] M. Talhavini, T.D.Z. Atvars, J. Photochem. Photobiol. A 114 (1998) 65.
[14] M. Talhavini, T.D.Z. Atvars, J. Photochem. Photobiol. A 120 (1999) 141.
[15] R.S. Davidson, K.R. Trethewey, J. Am. Chem. Soc. 98 (1976) 4008.
[16] C. Pizzocaro, R.A. Lessard, M. Bolte, Can. J. Chem. 76 (1998) 1746.
[17] D. Dibbern-Brunelli, T.D.Z. Atvars, J. Appl. Polym. Sci. 55 (1995) 889.
[18] D. Dibbern-Brunelli, T.D.Z. Atvars, J. Appl. Polym. Sci. 58 (1995) 779.
[19] D. Dibbern-Brunelli, T.D.Z. Atvars, I. Joekes, V.C. Barboza, J. Appl. Polym. Sci. 69 (1998) 645.
[20] E.G. Granados, J. Gonçalves-Benito, J. Baselga, D. Dibbern-Brunelli, T.D.Z. Atvars, I. Esteban, I.F. Pierola, J. Appl. Polym. Sci. 000 (2001).
[21] E.A. Turi, Thermal Characterization of Polymer Materials, Academic Press, New York, 1981.
[22] M. Talhavini, T.D.Z. Atvars, Quím. Nova 18 (1995) 298.
[23] D. Dibbern-Brunelli, T.D.Z. Atvars, J. Appl. Polym. Sci. 75 (2000) 815.
[24] V. Kasche, L. Lindqvist, J. Phys. Chem. 68 (1964) 817.
[25] J.B. Birks (Ed.), Organic Molecular Photophysics, Vol. 2, Wiley, Bristol, UK, 1975, p. 153.
[26] J.C. Hoockes, J.M. Torkelson, Macromolecules 28 (1995) 7683.
[27] M. Talhavini, T.D.Z. Atvars, C. Cui, R.G. Weiss, Polymer 37 (1996) 4365.
[28] J. Paczkowski, B. Paczkowska, D.C. Neckers, J. Photochem. Photobiol. A 61 (1991) 131.
[29] S.P. McGlynn, T. Azumi, M. Kinoshita, Molecular Spectroscopy of the Triplet State, Prentice-Hall, Princeton, NJ, 1979.
[30] R.S. Davidson, K.R. Trethewey, J. Am. Chem. Soc. 98 (1976) 4008.
[31] K. Kimura, T. Miwa, M. Imamura, Bull. Chem. Soc. Jpn. 43 (1970) 1329.
[32] N. Capolla, R.A. Lessard, Appl. Opt. 30 (1991) 1196.